Ministry of Education and Science of Ukraine

Odessa National Academy of Food Technologies

International Competition of Student Scientific Works

BLACK SEA SCIENCE 2021

Information Technology, Automation and Robotics

Proceedings

Odessa, ONAFT 2021

UDC 004.01/08

Black Sea Science 2021: Proceedings of the International Competition of Student Scientific Works. Information Technology, Automation and Robotics. / Odessa National Academy of Food Technologies; B.Yegorov, M. Mardar, S.Kotlyk (editors-in-chief.) [*et al.*]. – Odessa: ONAFT, 2021. – 526 p.

These materials of International Competition of Student Scientific Works «Black Sea Science 2021» contain the works of the contest participants in the section «Information technologies, automation and robotics» (not winners).

The author of the work is responsible for the accuracy of the information.

Odessa National Academy of Food Technologies, 2021

Organizing committee:

Prof. Bogdan Iegorov, D.Sc., Rector of Odessa National Academy of Food Technologies, Head of the Committee

Prof. Maryna Mardar, D.Sc., Vice-Rector for Scientific and Pedagogical Work and International Relations of Odessa National Academy of Food Technologies, Deputy Head of the Committee

Prof. Stefan Dragoev, D.Sc., Vice-Rector for Scientific Work and Business Partnerships of University of Food Technologies (Bulgaria)

Prof. Baurzhan Nurakhmetov, D.Sc., First Vice-Rector of Almaty Technological University (Kazakhstan)

Prof. Mircea Bernic, Dr. habil., Vice-Rector for Scientific Work of Technical University of Moldova (Moldova)

Prof. Jacek Wrobel, Dr. habil., Rector of West Pomeranian University of Technology (Poland)

Prof. Michael Zinigrad, D.Sc., Rector of Ariel University (Israel)

Dr. Mei Lehe, Ph.D., Vice-President of Ningbo Institute of Technology, Zhejiang University (China)

Prof. Plamen Kangalov, Ph.D., Vice-Rector for Academic Affairs of "Angel Kanchev" University of Ruse (Bulgaria)

Dr. Alexander Sychev, Ph.D., Assoc. Professor of Sukhoi State Technical University of Gomel (Belarus)

Dr. Hanna Lilishentseva, Ph.D., Assoc. Professor, Head of the Department of Merchandise of Foodstuff of Belarus State Economic University (Belarus)

Prof. Heinz Leuenberger, Ph.D., Professor of the Institute of Ecopreneurship of University of Applied Sciences and Arts (Switzerland)

Prof. Edward Pospiech, Dr. habil., Professor of the Institute of Meat Technology of Poznan University of Life Sciences (Poland)

Prof. Lali Elanidze, Ph.D., Professor of the Faculty of Agrarian Sciences of Iakob Gogebashvili Telavi State University (Georgia)

Dr. V. Kozhevnikova, Ph.D., Senior Lecturer of the Department of Hotel and Catering Business of Odessa National Academy of Food Technologies, Secretary of the Committee

The jury for the section
«Information technologies, automation and robotics»

Head of the jury:

Sergii Kotlyk – Ph.D., Associate Professor, Director of the P.M. Platonov Educational-Scientific Institute of Computer Systems and Technologies "Industry 4.0" of Odessa National Academy of Food Technologies (Ukraine)

Members of the jury:

Piotr Artiemjew - Dr hab., Associate Professor in Decision Systems of the Faculty of Mathematics and Computer Science,University of Warmia and Mazury in Olsztyn (Poland)

Francisco Antonio Augusto – Dr., International Relations Manager of Higher Institute of Information and Communication Technologies (Angola)

Andrey Kuprijanov – Ph.D., Associate Professor of the Department of Software for Computers and Automated Systems of Belarusian National Technical University (Belarus)

Simon Milbert – Vice-President of Xtra Information Management, Inc. (USA)

Ivan Palov – D.Sc., Professor of University of Ruse "Angel Kanchev" (Bulgaria)

Degla Gérard Hugues – Communications and Training Manager of "MAPCOM solutions informatiques" company group (Benin)

Nugzar Kereselidze - Academic Doctor of Informatics (Computer Science), Associate Professor of the Department of Natural Sciences, Mathematics, Technology and Pharmacy, Sukhumi State University (Georgia)

Etibar Seyidzade - Associate Professor of the Department of Computer and Information Technolohies, Baku Engineering University (Azerbaijan)

Vladimir Golenkov, D.Sc., Professor of the Department of Intelligent Information Technologies, Belarusian State University of Informatics and Radio Electronics (Belarus)

Zhanar Omirbekova - Ph.D., Associate Professor of the Department of Automation and Management, Satbayev University (Kazakhstan)

Ivan Palov - D.Sc., Professor of the Department of Power Supply and Electrical Equipment, University of Ruse "Angel Kanchev" (Bulgaria)

Siarhei Palavenia - Ph.D., Associate Professor, Head of the Department of Telecommunication Systems, Belarusian State Academy of Communications (Belarus)

Alexander Goloskokov - Ph.D., Professor of the Department of Software Engineering and Information Technology Management, National Technical University "Kharkiv Polytechnic Institute" (Ukraine)

Peter Nikolyuk - D.Sc., Professor of the Department of Computer Technology, Vasyl Stus Donetsk National University (Ukraine)

Vladimir Palagin - D.Sc., Professor, Head of the Department of Radio Engineering, Telecommunications and Robotics Systems, Cherkasy State Technological University (Ukraine)

Viktor Khobin – D.Sc., Professor, Head of the Department of Technological Processes Automation and Robotic Systems of Odessa National Academy of Food Technologies (Ukraine)

Valeriy Plotnikov – D.Sc., Professor, Head of the Department of Information Technology and Cybersecurity of Odessa National Academy of Food Technologies (Ukraine)

Sergii Artemenko – D.Sc., Professor, Head of the Department of Computer Engineering of Odessa National Academy of Food Technologies (Ukraine)

Fedir Trishyn - Ph.D., Associate Professor, Vice-Rector on Scientific and Educational Work, Odessa National Academy of Food Technologies (Ukraine)

Valerii Levinskyi – Ph.D., Associate Professor of the Department of Technological Processes Automation and Robotic Systems of Odessa National Academy of Food Technologies (Ukraine)

Viktor Yehorov – Ph.D., Supervisor of the Laboratory of Mechatronics and Robotics of Odessa National Academy of Food Technologies (Ukraine)

Pavlo Lomovtsev – Ph.D., Associate Professor of the Department of Information Technology and Cybersecurity of Odessa National Academy of Food Technologies (Ukraine)

Yurii Kornienko – Ph.D., Associate Professor of the Department of Information Technology and Cybersecurity of Odessa National Academy of Food Technologies (Ukraine)

Serhii Shestopalov – Ph.D., Associate Professor of the Department of Computer Engineering of Odessa National Academy of Food Technologies (Ukraine)

Anatoly Galiulin - Ph.D., Associate Professor, Acting Head of the Department of Electromechanics and Mechatronics, Odessa National Academy of Food Technologies (Ukraine)

Secretary of the jury:

Oksana Sokolova – Senior Lecturer of the Department of Information Technology and Cybersecurity of Odessa National Academy of Food Technologies (Ukraine)

AUTOMATIC NAIL TRANSFER TO THE IMM ZONE SYSTEM

Authors: ***Natallia Unarava, Aleksey Pronchak***
Advisors: ***Andrey Tyavlovsky, Alexander Isaev***
Belarusian National Technical University(Republic of Belarus)

Abstract. *The work describes the development stages and automatic nail transfer to the IMM zone system functioning concept.*
Keywords: *molding, thermoplastics, STM32, nails, automatic.*

I. INTRODUCTION

Injection molding machine (IMM) also known as an injection press, is a machine used for the thermoplastics parts manufacturing by injection molding. Currently, more than a third of the world's single-piece products from polymer materials are produced using injection molding machines. The injection molding technology is ideally suited to the mass production of complex shapes, an important requirement for which is exact size matching.

The cycle time in the casting process varies widely - thin-walled products can be produced in a few sonds, castings weighing hundreds of kilograms can be produced in minutes.

Plastics remain one of the most popular materials used in almost any area of technology and medicine. This is one of the most common methods. The main reason for its prevalence is the injection molding machine low cost with the ability to obtain any geometric shape products . Metal, wood or glass are significantly more expensive, so they can compete with polymer materials only in narrow niches. By using IMM you are allowed to automate the manufacturing process as much as possible, to obtain high-precision products at a low cost.

This process automation takes place, since injection molding technology has many advantages over other methods. Let's list the most significant of them:

-minimum waste;

-high performance;

-accelerated technological process;

-the ability to make polymer products with any shape and size [1].

The use of manual labor when using injection molding machines is minimal, all operations are controlled by automation, controlling all casting processes and the amount of material.

Products from polymer raw materials are widespread due to their low cost, high manufacturability of production, and the possibility of recycling.

For many types of manufacturing, it will be beneficial to organize such process on their own, and not buy them on the side.

There is nothing complicated to organize a line for the thermoplastic products manufacturing.

The inner mold contours precisely follow the future product shape, therefore, the complete filling of the tooling with polymer means obtaining geometrically accurate parts.

II. LITERATURE ANALYSIS

For the manufacturing owner automatic process is the most important, when all operations are controlled by electronics. The IMM elements are usually driven by a pneumatic drive, which is powered by an electric motor.

To avoid destroying the nails head, we cover them tightly with plastic. This way the nail will retain its aesthetic and will last longer as a construction component.

An automation of the transfer nails to the IMM zone process, this will significantly increase the number of processed nails per unit of time. Also we will receive a quality increase, since the transfer process will be fully and completely operated by the controller.

Block-schematic diagram is shown on the Fig. 1. It contains the following blocks:

- transfer controller;
- carriage transfer block;
- indicator;
- component transfer block;
- vibrodrive block;
- IMM;
- terminal block;
- manual controls and setting block.

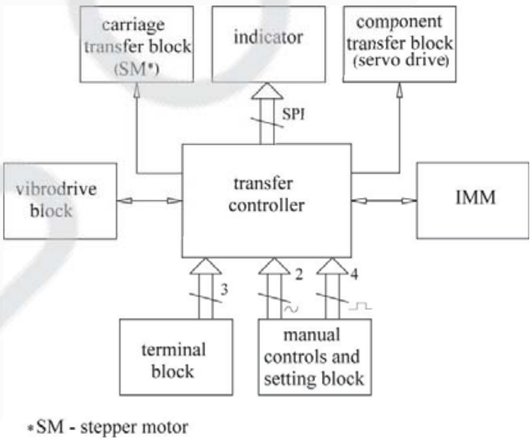

Fig. 1. Block-schematic diagram

Transfer controller is responsible for generating an appropriate signals at appropriate times. It analyzes button positions, sets transfer and mounting rate, changes system states and modes. Carriage trasfer block is a stepper motor unit. It’s responsible for keeping each nail fixed at appropriate place and transfering itself to IMM. Components transfer block inserts each nail to apropriate place. Indicator shows system modes. Terminal block is a device that opens a circuit in a system when moving parts reach their end position. Manual controls and setting block are used for transfer and mounting rate input. IMM covers each nail tightly with plastic.

General algorithm is shown on the Fig. 2. It contains steps to reach operating mode.

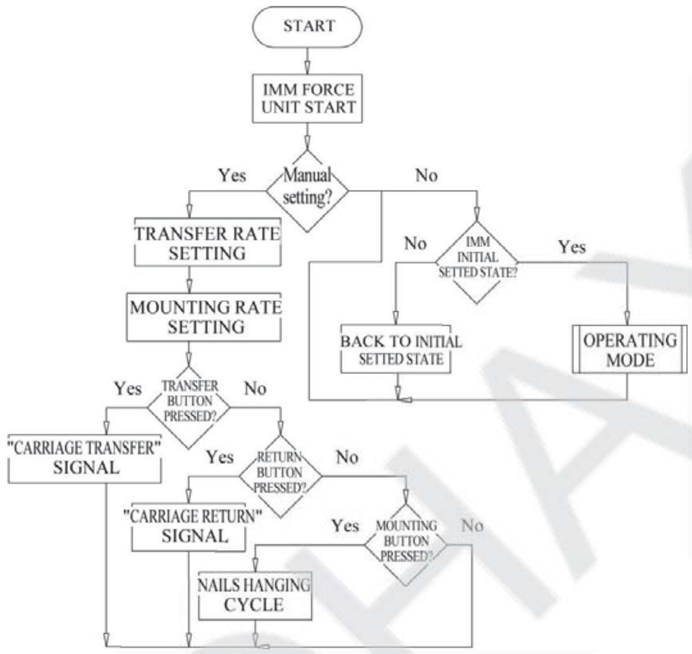

Fig. 2. General algorithm

Originally we launch IMM, we launch IMM force unit too. The controller checks for setting mode occurrence, is it manual. If it's happened, as result we receive transfer rate setting and mounting rate setting pollling. These steps we setting the system.

After the controller analyze if the transfer button is pressed. Pressed - a «carriage transfer» signal is generated by the controller. After the system goes for initial state check. Not pressed - the controller analyzes if the carriage return button is pressed. Pressed - a «carriage return» signal is generated. Not pressed - the controller checks for mounting button position. Pressed - the sustem goes to nails hanging cycle. Else - all goes back to setting.

The system is also checking itself for being in the initial setted state before the transfer process. When it's a step checks IMM initial setted state, in positive case, all goes to operating mode. Else the system is getting to initial setted state.

The operating mode includes transfer nails into the IMM zone according settings.

After the operating mode the controller checks for the system being in the initial setted state to continue performing in that mode.

Operating mode exicution algorithm is shown on the Fig. 3. Unlike general algorithm, this one demonstrates operating mode steps only.

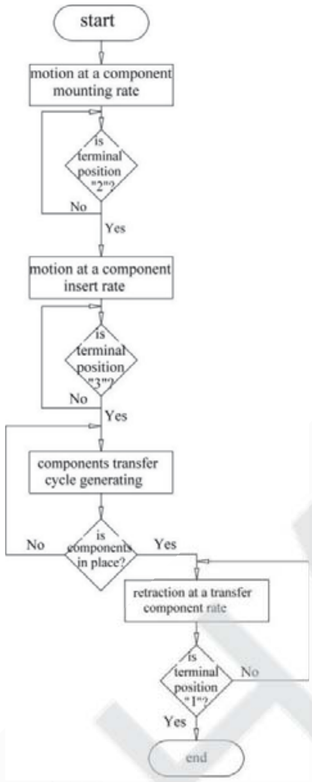

Fig. 3. Operating mode exicution algorithm

The controller tells everything to go at a component mounting rate before the terminal swithces to position “2”. This is for rate matching. After that, the motion takes a component insert rate value.

If the terminal is switched to “3” position, the controller generates a component transfer cycle. Which means components transfer to the IMM zone.

All components have to be placed into right apropriate places at the zone. When everything is correct, the controller tells the system to start retraction at a transfer component rate. It continues until the terminal position is “1”. It means that every component is in the IMM zone now.

III. ELEMENT BASE DECISION AND REASON

3.1. Microcontroller

To implement the control unit, it is advisable to use the debug board based on the popular and cheap STM32F103C8T6 microcontroller.

The debug board contains the STM32F103C8T6 microcontroller, as well as a voltage regulator, which provides the microcontroller with a stable 3.3 V power supply, which is necessary for a correctly working controller. In addition to the above, the board has an external crystal oscillator, two LEDs, one of which is a power supply indicator, and the other is a test one. Pins of the microcontroller, including pins for programming, are brought out to the edges of the board for easy wiring.

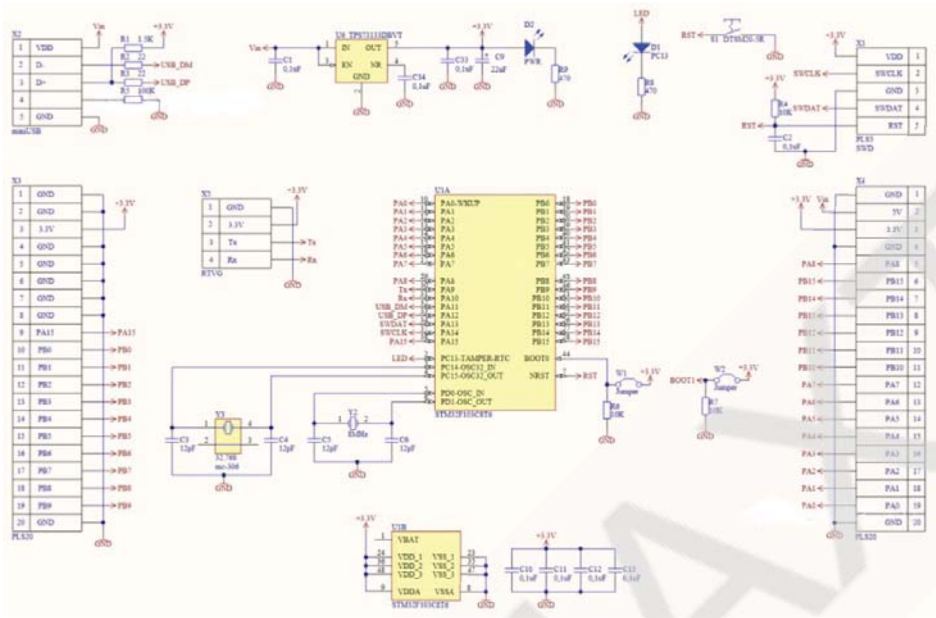

Fig. 4. The debug board based on the STM32F103C8T6 microcontroller

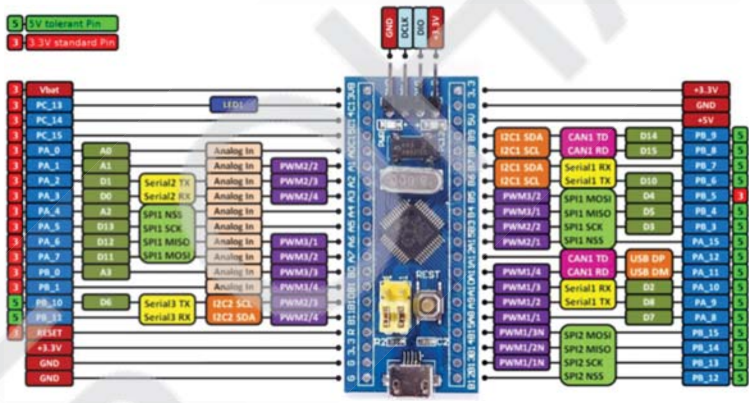

Fig. 5. The debug board based on STM32F103C8T6 appearance

The STM32F103C8T6 is a low-power high-performance microcontroller. It can be powered by a 2 V voltage power supply with a 72 MHz core clock while all peripherals enabled and still only draw 36mA. In power saving mode, the STM32 consumes 2 μA.

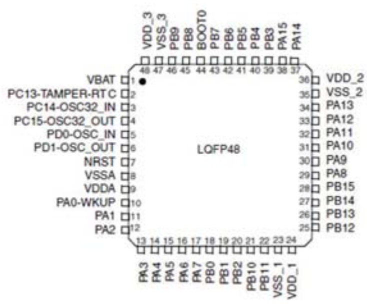

Fig. 6. STM32F103C8T6 pins

One of the requirements for modern devices is to ensure the safety of the program code from unauthorized access. Read protection through the debug port can be set for STM32 flash memory. While read protection is enabled, flash memory is also write protected to prevent the possibility of incorrect code being placed in the interrupt vector table. STM32 microcontrollers also contain a real time clock and a small amount of battery-powered SRAM. The contents of this area are automatically cleared by an interrupt from the anti-tampering module.

The STM32 requires a single power supply with a voltage ranging from 2.0 V to 3.6 V. The onboard regulator is used to generate 1.8 V for the Cortex core. STM32 can have two additional power supplies. When using an ADC, the VDD power supply voltage must be between 2.4 V and 3.6 V. The 48-pin packages the reference signal is internally connected to the ADC power supply pin. Each voltage source must have stabilizing capacitors.

The STM32 is well equipped with general purpose GPIO I/O ports. They are grouped as five ports, each containing 16 I / O lines. Each digital pin can be configured as a GPIO pin or as an alternative function pin. Each pin can simultaneously operate as one of 16 external interrupt lines.

Ports are designated from A to E latin alphabet and all are 5 V tolerant. Many of the external microcontroller pins can be switched to serve user peripherals such as the USART or I2C instead of performing I/O functions.

The individual pins of each GPIO port can be configured as input or output of various drivers. Ports contain registers into which you can write information in word format or manipulate their bit fields. After making the settings, the registers can be locked.

A port pin can be defined as input or output, and its load characteristic can be selected. If the pin is defined as an input, using the built-in register, you can "pull" the pin to ground or supply voltage. If the pin is defined as an output, it can be configured as push-pull or open-drain. Each output can also be configured to operate at frequencies up to 2 MHz, 10 MHz, or 50 MHz.

In addition to an excellent set of general-purpose peripherals, the STM32 contains five different types of communication peripherals. The STM32 contains SPI and I2C interfaces to exchange information between components on a printed circuit board. There is a CAN bus for communication between different modules of the device, and a USB device interface for communication with a PC. The STM32 also uses the popular USART interface.

For fast data exchange between PCB components, the STM32 contains two SPI modules that provide full duplex data transmission at frequencies up to 18 MHz. It is very important to note that one of the SPI modules is located on the high-speed APB2 peripheral bus, which operates at a clock frequency of up to 72 MHz. The sond SPI is located on the low speed APB1 bus, clocked at up to 37 MHz. For each SPI, you can set the clock polarity and phase. Data can be transmitted as 8 or 16-bit words, MSB or LSB. This allows both SPI modules to act as master or slave and communicate with any other SPI device.

To organize high-speed data exchange, each SPI module contains two DMA channels: one for transmitting data and the other for storing received data into memory. The use of DMA allows high speed data exchange in two directions under hardware control. In addition to the standard functions, the STM32 SPI contains two hardware blocks for calculating the cyclic redundancy code CRC. One CRC block is used for transmitted data, and the sond for received data. Both blocks can calculate cyclic redundancy check for 8 and 16-bit data. This function is especially necessary when connecting to SPI MMC/SD memory cards.

STM32 can communicate with other components on the PCB via I2C interface. The I2C interface can operate as a slave or master, and arbitrate in a multi-master system. The SPI interface supports standard data rates up to 100 kHz and fast data rates up to 400 kHz. The I2C module supports 7-bit and 10-bit addressing modes. Essentially, the I2C module simply transmits and receives data over the bus. The I2C module generates two interrupts for the Cortex processor, one to limit error propagation and one to control addresses and data transfers. In addition, two DMA channels are allocated through which you can read from and write data to the I2C transmit buffer. Thus, after coordinating the addresses of devices in the network and data for transmission, the exchange of information can be carried out under STM32 hardware control.

The STM32 contains up to three USARTs, each of which supports several advanced modes to work with modern serial devices. Each of the three USARTs can communicate at speeds up to 4 Mbps. For each USART, you can set the data length (8 or 9 bits), parity stop bit and baud rate. One USART is located on the APB2 bus, which runs at up to 72 MHz, while the rest are on the APB1 bus, which clocks at up to 36 MHz.

Like all other serial communications peripherals, each USART supports two DMA channels for transferring data to and from memory. When the USART is used as a UART, it supports several special communication modes. The USART can transmit data in half duplex mode over a single wire using only the Tx pin. For connecting a modem, as well as for hardware control of data transmission, each USART contains additional control lines CTS and RTS. At the same time, a transmission speed of up to 115200 bit/s is provided, half-duplex NRZ modulation is used, a low power consumption mode is supported when the USART module operates at frequencies from 1.4 MHz to 2.12 MHz.

The STM32 CAN controller is a full-fledged CAN module that supports the CAB 2.0A and 2.0B standards, active and passive data transfer at speeds up to 1 Mbit/s. The CAN controller also has an extension to support fully deterministic data exchange according to the TTCAN protocol. While the TTCAN extension is enabled, automatic message retransmission and message time stamping are supported in the last two bytes of a CAN message packet. The TTCAN extension enables the CAN module to be used by real-time control application software. An important feature of the CAN controller is the filtering of received messages. Since CAN is a broadcast network, every message transmitted is received by all devices on the network. In a CAN network of sufficient complexity, a large number of messages will be transmitted over the CAN bus. The CPU would have to spend all the time processing these messages. To avoid this, the CAN controller contains a message filter that prevents unnecessary messages from being copied into the receive buffer.

All CAN controllers support two modes of operation: normal mode, for receiving and transmitting message packets, and initialization mode, for setting communication parameters. STM32 can enter "sleep" mode. At such times, the bxCAN clock is disabled, but the mailbox registers may remain available. The bxCAN module will wake up when it detects activity on the CAN bus; it can also be resumed from the application code. In normal mode, there are two sub-modes of operation. The first submode is the silent mode, in which the CAN controller receives but does not transmit messages, and also does not generate an error or message acknowledgment. This mode is intended for passive monitoring of the CAN network. The sond submode is the feedback mode, in which all transmitted messages are returned to the receive buffer. This mode is intended for self-testing and is also used when debugging the application code. Both sub-modes can be combined, which is ideal for self-testing a device in a working network.

STM32 contains a full speed (12 Mbps) device USB interface that can be used to connect the device to a PC. The USB module implements the USB physical layer and the data transfer layer with packet error checking and retransmission. The USB interface supports up to eight endpoints, which the user configures as control, interrupt, bulk, and isochronous endpoints. The endpoint buffers are located in a 512 byte SRAM area shared with the CAN controller. During device initialization, the application code splits the SRAM into buffer groups. The SRAM memory area is divided into endpoint buffers using a special table located at the beginning of the SRAM. For each endpoint, the table stores the start address and buffer size. One buffer is allocated for endpoints operating in control mode, interrupts, and large data transfers, while a double buffer is allocated for isochronous endpoints. This allows you to receive data into one buffer and simultaneously process data from another.

3.2. DC motor shaft speed and direction control circuit

To control the DC motor shaft speed and movement direction, we used a circuit coupled with a control unit based on the IRS2186 microcircuit of the 74HCT08 logic gate and the FGH60N60SMD transistor.

The 8-pin SOIC IRS2186 is a high voltage, high speed MOSFET and IGBT driver with independent output channels. Patented anti-latching HVIC and CMOS technologies provide a solid monolithic design.

The logic input is compatible with standard CMOS or LSTTL output, up to 3.3 V logic.

The output drivers have a high surge current buffer stage designed to minimize driver cross-conduction.

The IRS2186 is a 600 V low and high level driver. The driver's output currents are ± 4 A, compatible with 3.3 V and 5 V control logic, undervoltage protection.

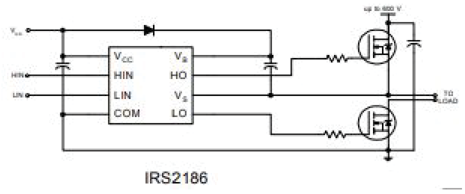

Fig. 7. IRS2186 driver connection diagram

In many cases, it becomes necessary to use field-effect transistors as top-level switches. Also, in many cases, there is a need for field-effect transistors as switches of both the upper and lower levels. For example, in bridge circuits.

In a half-bridge circuit, there is one high-level MOSFET and one low-level MOSFET. In bridge circuits, there are two MOSFETs each of the upper and lower levels. The most common way to drive FETs in such cases is to use a low and high key driver for the MOSFET.

Block diagram, as well the location of the contacts of a common driver IRS2186 for such purposes:

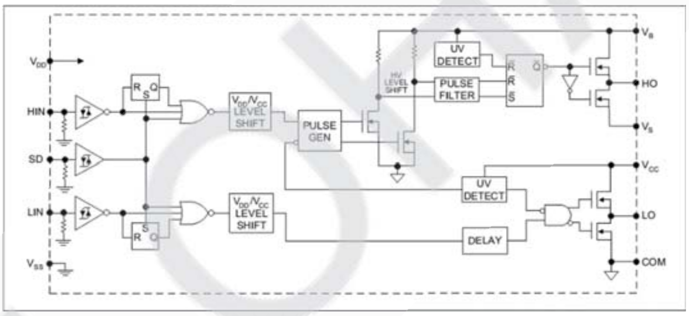

Fig. 8. IRS2186 functional block diagram

It's also worth mentioning that the IRS2186 comes in two packages - a 14-pin PDIP for pin mount and a 16-pin SOIC for surface mount.

VCC is the low level power supply, must be between 10 V and 20 V.

VDD is the logic power for the IR2110, it must be between + 3 V and + 20 V (relative to VSS). The actual voltage you choose to use depends on the voltage level of the input signals. The curve:

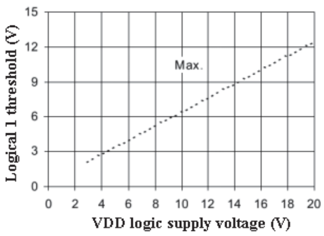

Fig. 9. Logical «1» power curve

Usually a + 5 V VDD is used. At VDD = + 5 V, the input threshold of logic 1 is slightly higher than 3 V. Thus, when VDD = + 5 V, the IR2110 can be used to drive a load when the «1» input is higher than 3 (somewhat) volts. This means that the IRS2186 can be used for almost all circuits, as most circuits tend to be powered by about 5 V. When you use microcontrollers, the output voltage will be higher than 4 V (after all, the microcontroller often has VDD = + 5 V). When a SG3525 or TL494 or other PWM controller is used, it will probably have to be supplied with a voltage above 10 V, which means that the outputs will be more than 8V with a logical «1». Thus, the IR2110 can be used almost anywhere.

It is also possible to lower VDD to about + 4 V if using a microcontroller or any chip that provides 3.3 V output (for example, dsFig33). In practice, good results are obtained by using the supply voltage + 5 V.

If for some reason in the circuit the level of the logic «1» signal has a voltage less than 3 V, then you need to use a level converter / level translator, it will raise the voltage to acceptable limits. In such, it is recommended to increase to 4 V or 5 V and use the IRS2186 VDD = + 5V.

VSS is the land for logic. COM is «low return» - basically the low ground of the driver.

HIN and LIN are logic inputs. A high signal on HIN means that we want to control the high key, that is, a high level is output to HO.

A low signal on HIN means that it is necessary to turn off the high-level MOSFET, that is, a low-level output is made on the HO. The HO output, high or low, is not considered to ground, but to VS. At a high level, the level at HO is equal to the level at VB, with respect to VS. At a low level, the level at HO is VS, in relation to VS, virtually zero.

A high LIN signal means that it is necessary to drive the lower switch, that is, a high level output is made to LO. A low LIN signal means that it is necessary to turn off the low level MOSFET, that is, a low level output is carried out on LO. The exit to LO is relative to ground. When the signal is high, the level in LO is the same as in VCC, relative to the VSS, effectively ground. When the signal is low, the level in LO is the same as in VSS, relative to VSS, effectively zero.

SD is used as stop control. When the level is low, the IR2110 is enabled - the stop function is disabled. When this pin is high, the outputs are turned off, disabling the IRS2186 control.

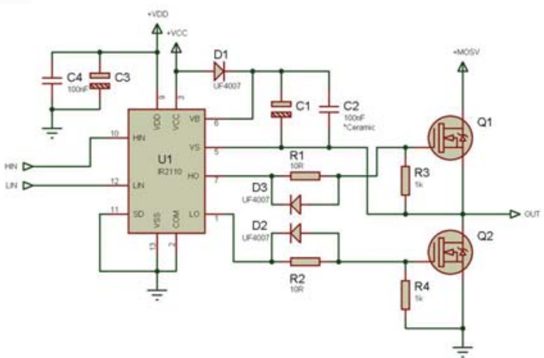

Fig. 10. IRS2186 half-bridge control diagram

D1, C1 and C2 with the IRS2186 form an amplifier circuit. When LIN = 1 and Q2 is on, then C1 and C2 are charged to VB, since one diode is located below + VCC. When LIN = 0 and HIN = 1, the charge on C1 and C2 is used to add additional voltage, VB in this case, above the Q1 source to drive Q1 in the high-key configuration. A large enough capacity must be chosen for C1 in order for it to be sufficient to provide the necessary charge for Q1 to keep Q1 on the entire time. C1 should also not have too much capacity, as the charging process will take a long time and the voltage level will not increase enough to keep the MOSFET on. The longer the time it takes in the on state, the more capacity is required.

Thus, a lower frequency requires a higher C1 capacity. Higher fill factors require higher capacities C1. Of course, there are formulas for calculating the capacity, but for this you need to know many parameters, and some of them we may not know, for example, the leakage current of a capacitor. Therefore, we just estimated the approximate capacity. For low frequencies such as 50Hz, a capacitance of 47 µF to 68 µF is used.

For high frequencies, such as 30-50 kHz, I use a capacitance of 4.7 µF to 22 µF. Since an electrolytic capacitor is used, a ceramic capacitor must be used in parallel with this capacitor. A ceramic capacitor is optional if the booster capacitor is tantalum.

D2 and D3 discharge the gate of the MOSFETs quickly, bypassing the gate resistors and reducing the turn-off time. R1 and R2 are current limiting gate resistors. + MOSV can be 500V maximum. + VCC should come from a source without interference. Filtering capacitors are also required.

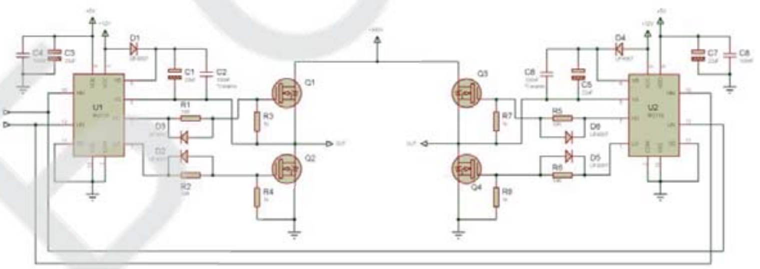

Fig. 11. Applied circuit

Fig. 12. FGH60N60SMD transistor

FGH60N60SMD transistor parameters:
- Maximum voltage – 600 V
- Maximum current at 25°C – 120 A
- Peak transistor collector current – 180 A
- Saturation voltage – 2.5 B

- Power dissipation rating – 600W
- On-delay time at 25°C – 12 ns
- Off-delay time at 25°C – 92 ns

3.3. The switching relay module

The relay switch TR5VL-S-Z is intended for switching the TI unit to the measuring circuit.

Fig. 13. The relay switch TR5VL-S-Z

The switching relay module is a set of miniature telecommunication relays capable of providing reliable contact at low switching currents (from 1 μA to 2 A). One switch can connect eight two-wire measurement circuits. The switch occupies one «terminal» position and has spring-loaded connectors for connecting switching and control circuits.

3. 4. The matching the signal levels of the control unit and the load circuit

To match the voltage level received from the inductive sensors and the voltage level that the output port of the STM32F103C8T6 microcontroller is used a galvanic isolation scheme based on the PC817 optical pair.

The PC817 is a widely used optocoupler from Sharp. Internally, the optocoupler consists of an LED and a phototransistor, which are not electrically connected in any way, thanks to which, on the basis of PC817, it is possible to realize galvanic isolation of two parts of the circuit - for example, signal and power.

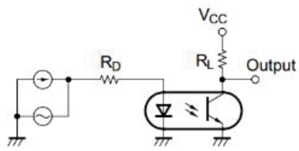

Fig. 14. PC817 connection diagram

PC817 parameters:
- I/O insulation maximum voltage – 5000 V
- Maximum forward current – 50 μA
- Collector- emitter maximum voltage – 35 V
- Power dissipation rating – 150 mW
- Maximum throughput frequency – 80 kHz

3.5. Transistor switch

Field-effect transistors of the MOSFET family are used as transistor switches in the circuit: IRFR024 and IRLML2060TRPbF.

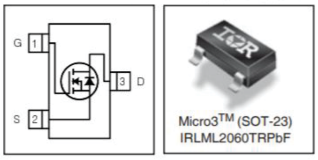

Fig. 15. IRLML2060TRPbF transistor

IRLML2060TRPbF parameters:
- Structure – n-channel
- Source-drain maximum voltage – 60 V
- Source-drain maximum current – 1.2 A
- Gate-source maximum voltage – 16 V
- RDSon – 0.48 Ω at 1.2 A, 10 V
- Power dissipation rating – 1.25 W
- Gate threshold voltage – 1…2.5V

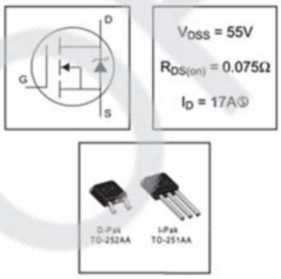

Fig. 16. IRFR024 transistor

IRFR024 parameters:
- Structure – n-channel
- Source-drain maximum voltage – 55 V
- Source-drain maximum current – 17 A
- Gate-source maximum voltage – 20 V
- RDSon 0.075 Ω at 10 A, 10 V
- Power dissipation rating – 45V

IV. RESULTS

To implement the control scheme, the following blocks were designed:
- transfer controller;
- switching relays module;
- DC motor control unit;
- manual controls connection block;
- display unit;

- inductive sensors and optical isolation connecting block.

Control board general view is shown in Fig. 17.

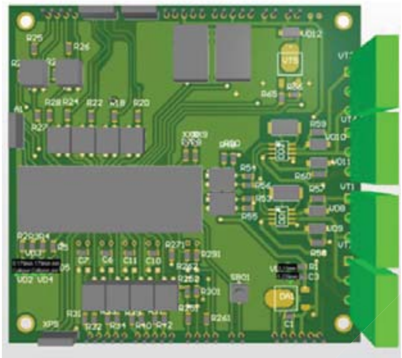

Fig. 17. Control board general view

The device is controlled using a debug board based on the STM32F103C8T6 microcontroller.

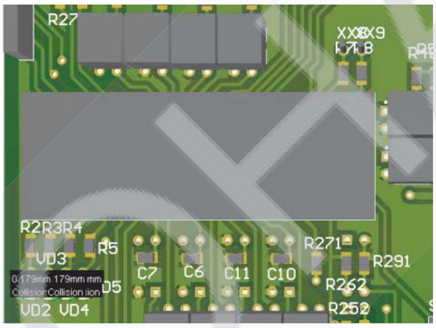

Fig. 18. STM32F103C8T6 debug board location on the control board

The relay switches are controlled by the microcontroller outputs of the control unit. Their placement on the board is shown in Fig. 19.

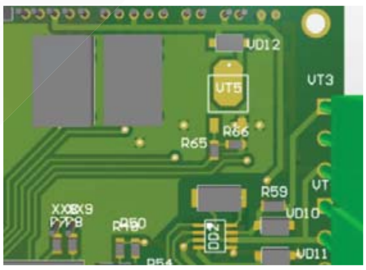

Fig.19. Relay switches location on the control board

The DC motor control unit is implemented using IR2186 high-voltage high-speed drivers and FGH60N60 high-voltage transistors. This circuit is controlled by control unit outputs. The location of the DC motor control unit is shown in Fig.20.

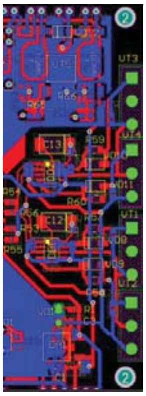

Fig. 20. The DC motor control unit location on the control board

Block with detachable interface expander for display connection.

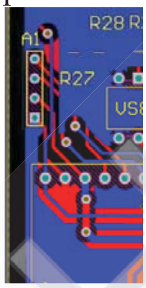

Fig. 21. Display connection

The inductive sensors and optical isolation block is implemented using inductive sensors and PC817 optical pairs. Optical isolation is required to match the level of the signal arriving at the microcontroller input of the control unit and the output signal of inductive sensors. The location of the optically isolated inductive sensor block on the control board is shown in Fig. 22.

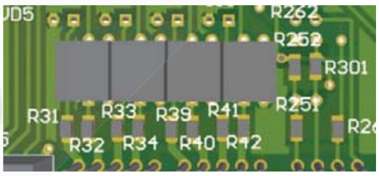

Fig. 22. The inductive sensors and optical isolation block location on the control board

V. CONCLUSIONS

The developed line is installed at the closed stock company "EKT" production association for covering nails with thermoplastic.

VI. REFERENCES

1. Douglas M. Plastic Injection Molding: Manufacturing Process Fundamentals / M. Douglas. – SME, 1996. – P. 11

2. The line for the production of gypsum plasterboard profiles (KNAUF system):https://meer.group/liniya-dlya-proizvodstva-profilej-dlya-montazha-gipsokartonnyix-plit

International Competition of Student Scientific Works

BLACK SEA SCIENCE 2021

Information Technology, Automation and Robotics

Proceedings

Odessa National Academy of Food Technologies

The collection includes student works of the participants of the competition, which were not included in the number of prize-winners. The texts of the competitive works are published in the form in which they were submitted by the authors. The authors of the articles are responsible for the content and form of submission of the material.

Responsible for the issue: Sergii Kotlyk

Computer typesetting and layout: Oksana Sokolova

Odessa 2021